Contents lists available at GrowingScience

Current Chemistry Letters

homepage: www.GrowingScience.com

A novel chitosan-coated neem flower bio-adsorbent for the removal of methylene blue dye from wastewater: Thermodynamics, isotherm and kinetic studies

P. Jeevan Kumar[a], S. Induja[a], P.S. Raghavan[a], B. Gajalakshmi[a] and V. Parthasarathy[b*]

[a]*Department of Chemistry, Hindustan Institute of Technology and Science, Padur, Chennai – 603 103, India*
[b]*Department of Physics, Hindustan Institute of Technology and Science, Padur, Chennai – 603 103, India*

C H R O N I C L E

Article history:
Received February 3, 2022
Received in revised form
April 8, 2022
Accepted May 18, 2022
Available online
May 18, 2022

Keywords:
BET
Bio-adsorbent
Methylene blue dye
Wastewater
FTIR

A B S T R A C T

The chitosan-coated neem flower powder was prepared and employed as an adsorbent for the removal of cationic methylene blue from an aqueous medium. The interaction of chitosan with neem flower was concluded by FTIR. The BET surface area was evaluated for the prepared NFC adsorbent. The adsorption of methylene blue dye onto chitosan-coated neem flower powder (bio-adsorbent) was carried out by varying the concentration of dye, pH, temperature and concentration of adsorbent. The adsorption capacity was evaluated by using Freundlich and Langmuir models. The adsorption data were further analysed with the help of pseudo-first and second-order kinetic models. The thermodynamic parameters were evaluated to comprehend the nature of the adsorption process.

1. Introduction

Environmental pollution is a worldwide threat to all forms of life since that imposes severe effects on plants, human health, animals and aquatic life. The discharging of industrial and organic effluents into a landfill drastically increases soil and water pollution. Discharge of dyes brings about severe damage to environment.[1-4] Various techniques like coagulation-flocculation, nano-filtration and chemical precipitation are adopted to remove the hazardous dyes from the textile effluents.[5,6] However, these techniques have their own shortcomings in terms of colour removal, high cost and production of secondary sludge. Therefore, adsorption is a promising technique in the removal of dyes as it overcomes the shortcomings of other techniques.

The removal of cationic methylene blue dye is quite challenging from the effluent owing to its complex aromatic structure. Bu *et al.*[7] studied the adsorption of methylene blue by thiosemicarbazide-graphene composite. The adsorption efficiency of biochar/polysulfone membrane was assessed towards the removal of methylene blue.[8] The neem leaf powder was employed as an adsorbent on the removal of methylene blue under various experimental conditions by Krishna and his research team.[9] Adeleke *et al*.[10] investigated the photo-catalytic activity of the prepared $ZnO/NiFe_2O_4$ nanoparticle on the degradation of methylene blue. The methylene blue adsorption on the modified cellulose film was evaluated by Shi and his research team.[11] The evaluation of the adsorption capacity of neem leaf powder on the removal of methylene blue was carried out by using Freundlich and Langmuir isotherm.[12] The biosorbent of neem bark on the removal of dye was studied, and thermodynamic parameters associated with adsorption of dye were also evaluated by Srivastava and his co-workers.[13] The liquid-phase adsorption of methylene blue and indigo carmine was reported to be increased while increasing the

* Corresponding author.
E-mail address: parthu0406@gmail.com (V. Parthasarathy)

doi: 10.5267/j.ccl.2022.5.004

biosorbent concentration of neem bark in the literature.[14] Further studies on the removal of methylene blue from wastewater were carried out by various research groups.[15-21]

In the present investigation, chitosan acts as an adsorption promoter due to the presence of hydroxyl and amino groups. These groups are expected to get activated on varying pH and that alters the adsorption process. Another novelty of the present investigation is the neem flower powder which is used as the adsorbent base. Till now, no report was available using the neem flower as the adsorbent. The soft texture and low density of neem flower powder as compared to neem leaves or neem tree bark favours its candidature in the present investigation. Thus, the prepared chitosan-coated neem flower (NFC) effectively adsorbed even at a higher initial concentration of dye from an aqueous medium due to the strong interaction between the hydroxyl groups of chitosan-modified neem flower and the cationic methylene blue dye.

2. Results and discussion

2.1. FTIR study

The FTIR spectra of the NF and NFC samples are given in **Fig. 1**. The general observation was that the vibration of both the samples was nearly the same and the intensity was less in NFC as compared to the NF sample. The characteristic fingerprint of chitosan (minor component) was not observed, due to the masking by the NF (major component). The vibration intensity corresponding to -OH (3400 cm^{-1}) and that corresponding to C-H (2900 cm^{-1}) was reduced in NFC as compared to NF suggesting strong interaction of chitosan with the NF.[22]

2.2. BET analysis

The BET analysis revealed that the surface area of the NFC has decreased as compared to the NF sample (**Table 1**). The pore volume was also found to be decreased. This would have resulted in a decrease in mean pore diameter. The chitosan was reported to be non-porous with low surface area and pore volume in literature.[23] Hence, it can be concluded from the above study that the chitosan has favored modification of the surface without much affecting the surface area and pore volume of NF during the preparation of NFC.

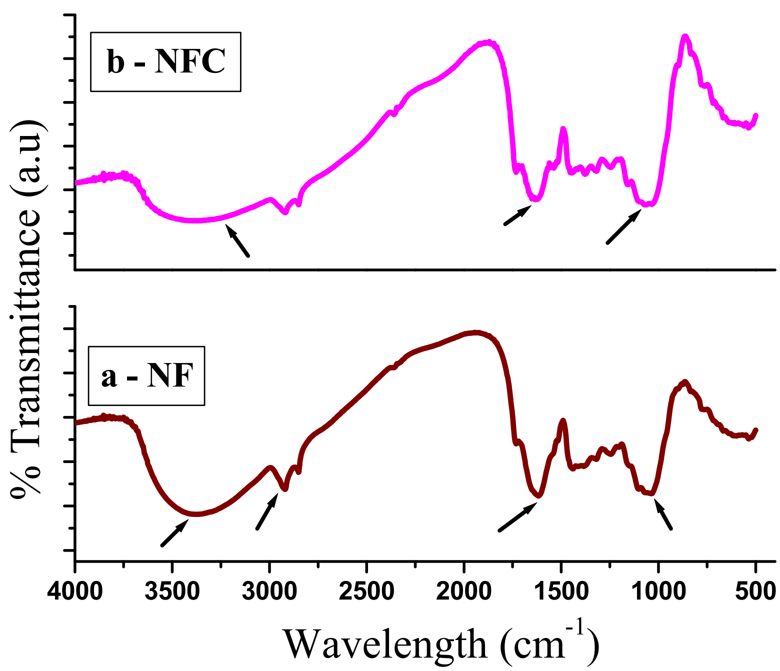

Fig. 1. FTIR spectra of a) NF and b) NFC

Table. 1. BET analysis results of NF and NFC samples

Sample	Volume adsorbed, V_m ($cm^3\ g^{-1}$)	Mean pore diameter (nm)	Total pore volume ($\times 10^{-3}\ cm^3\ g^{-1}$)	Surface Area, S_{BET} ($m^2\ g^{-1}$)
NF	0.1811	43.8	8.63	0.788
NFC	0.1512	41.2	6.79	0.656

2.3. Adsorption study

The chitosan contains hydroxyl and amino groups whereas methylene blue contains the ammonium group.[24] Hence, the adsorption process will be greatly influenced by the pH of the medium. In acidic pH, the amino groups will be protonated and may not favour adsorption, while, in an alkaline pH, the hydroxyl groups may be activated and favour adsorption.

The adsorption of the methylene blue dye from the solution with respect to time is given in **Fig. 2**. It can be seen that the equilibrium adsorption capacity of the NFC for the dye attained steady-state within 15 min of adsorption time, while the neem leaf powder was reported to attain equilibrium after 5 hours.[9]

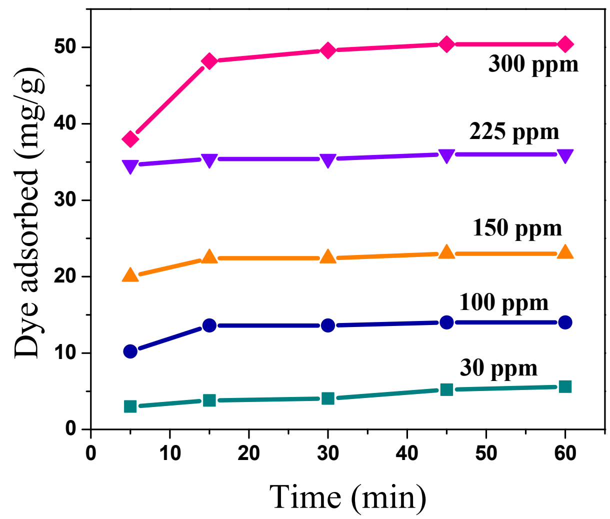

Fig. 2. Adsorption of different concentration of methylene blue with time

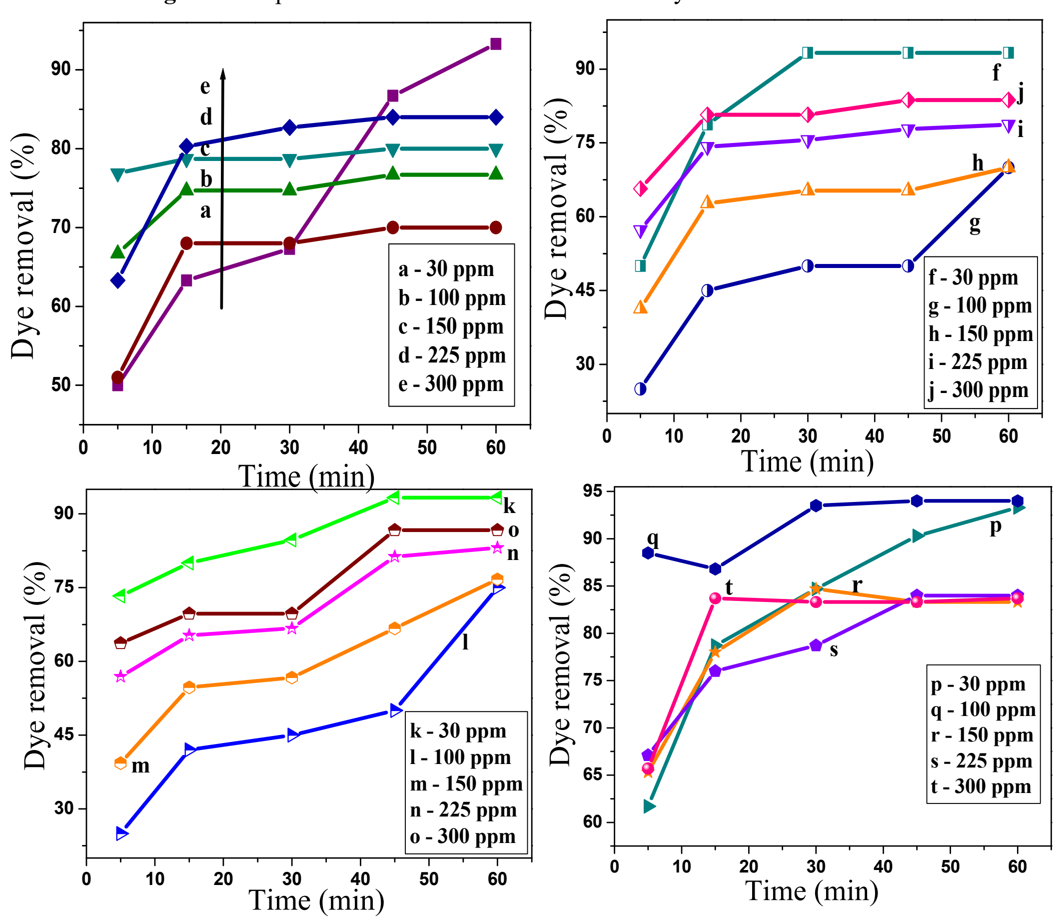

Fig. 3. Dye removal % for different concentrations of dye at a-e) 3 pH, f-j) 6 pH, k-o) 9 pH and p-t) 11 pH

The influence of initial dye concentration at pH of 3 was studied and the removal % of the dye is given in **Figs. (3a-e)**. Even though the removal % of the dye at 30 ppm was less initially, over a period of time, it reached the maximum. The high removal % of dye at high concentration is due to the more availability of dye and attains saturation earlier compared to low concentration of dye. On increasing the pH to 6.0, removal % at a dye concentration of 150 ppm and above reached saturation within 15 min, while that of 30 ppm was highest (**Figs. 3f-j**). The same trend was observed at pH = 9.0 as illustrated in **Figs. 3k-o**.

On further increasing the pH to 11, the dye concentration at 30 & 100 ppm was found to adsorb well but removal % decreased with an increase in dye concentration (**Figs. 3p-t**). This observation leads to the conclusion that dye adsorption is favoured in mild acidic and alkaline pH conditions.

The dye adsorption at 5 min and equilibrium adsorption at 60 min are given in **Figs. 4a-d** and 4e-h. The above observation can be confirmed that at 5 min, the pH 6 & 9 favours maximum adsorption while pH of 3 & 11 exhibits low adsorption. However, over a period of 60 min, the adsorption was found to follow nearly the same trend, irrespective of the pH of the medium.

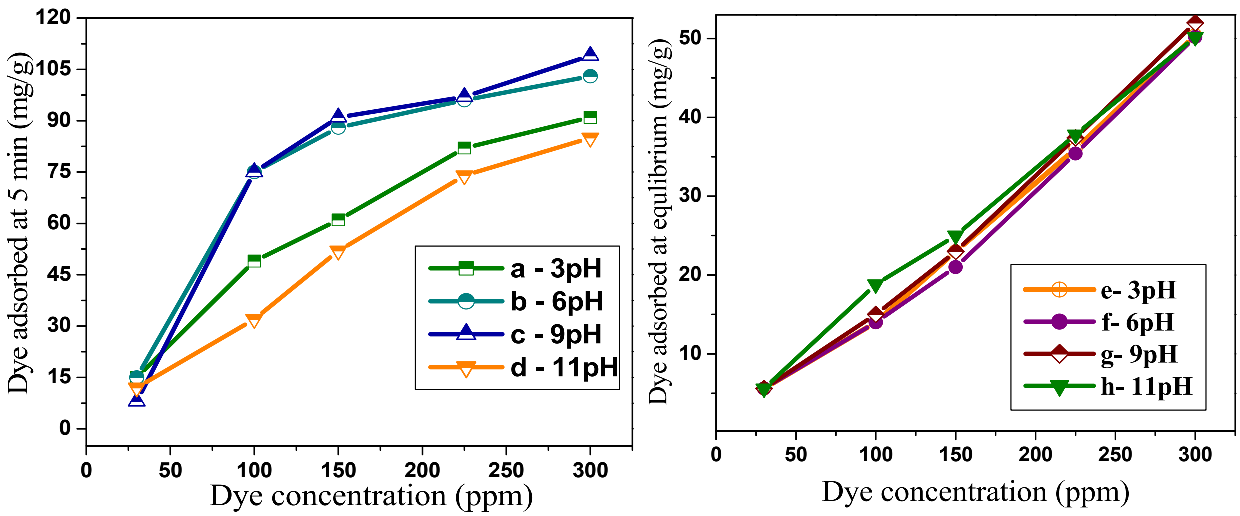

Fig. 4. Dye adsorption for different pH concentrations at a-d) 5 min and e-h) 60 min.

2.4. Adsorption isotherms

2.4.1 Langmuir adsorption model

According to the Langmuir adsorption model, the equilibrium adsorption of dye (q_e) is related to the concentration (C_e) in the medium by the following relation[25]:

$$\frac{1}{q_e} = \frac{1}{q_m} + \frac{1}{q_m K_L C_e}$$

Where q_m is the Langmuir monolayer adsorption capacity in mg/g and K_L is the equilibrium constant (L g^{-1}). The Langmuir plot of the adsorption data, i.e., $1/q_e$ Vs $1/C_e$ is given in **Fig. 5**. It can be seen from the plot that the adsorption of dye over NFC was nearly the same at all pH. The Langmuir adsorption capacity and equilibrium constant were calculated from the slope of the straight line and the intercept (**Table 2**).

Table. 2. Data of Langmuir Adsorption Model

	Equilibrium constant, K_L				R_L values			
Con. of dye, ppm	**3 pH**	**6pH**	**9pH**	**11pH**	**3 pH**	**6pH**	**9pH**	**11pH**
30	0.00165	0.00194	0.00130	0.00053	0.95	0.95	0.96	0.98
100	0.00133	0.00159	0.00112	0.00056	0.88	0.86	0.90	0.95
150	0.00160	0.00173	0.00122	0.00050	0.81	0.79	0.85	0.93
225	0.00193	0.00236	0.00149	0.00053	0.70	0.65	0.75	0.89
300	0.00245	0.00323	0.00179	0.00055	0.58	0.51	0.65	0.86
q_m (mg/g) =	102.0	119.0	149.0	357.0				

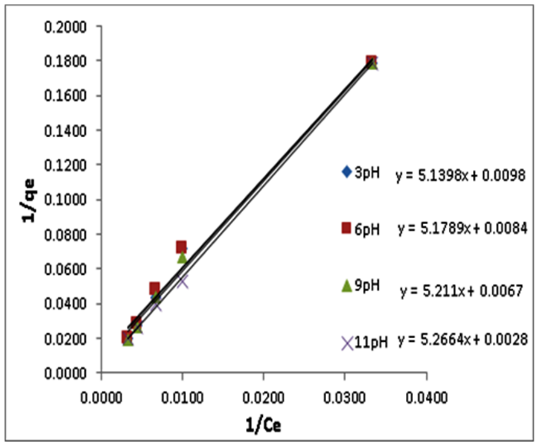

Fig. 5. Langmuir plot of adsorption for different concentration of pH

The monolayer adsorption capacity was found to increase with the pH of the medium, while the monolayer adsorption of methylene blue over neem leaf powder was around 19.62 mg/g and neem leaf-chitosan exhibited 102 mg/g.[9] A plot of K_L Vs concentration of dye[26] at different pH is illustrated in **Figs. 6a-d**. The equilibrium constant K_L was found to increase with an initial concentration of dye and the highest value was observed at pH=6, suggesting favourable adsorption of dye. One of the important Langmuir parameters, namely, R_L can be calculated from the equation.[27]

$$R_L = \frac{1}{1 + (K_L C_e)}$$

The value of R_L represents the nature of the interaction between the substrate and adsorbate. When the value of R_L is greater than 1, it indicates unfavourable adsorption, while, if the value is between 0 and 1, it indicates favourable adsorption. The R_L was calculated at different pH for different initial dye concentrations and the same is given in **Table 1**. From the Table, it can be seen that R_L was between 0 and 1 (0.5 – 0.95), suggesting that the methylene blue is irreversibly adsorbed on the NFC surface, while neem leaf-chitosan exhibited R_L value as low as 0.319.[33] A plot of R_L Vs concentration of dye at different pH is given in **Figs. 6e-h**. The R_L value was found to decrease with an increase in dye concentration and the variation was least at 11 pH and the lowest was observed at pH=6.0.

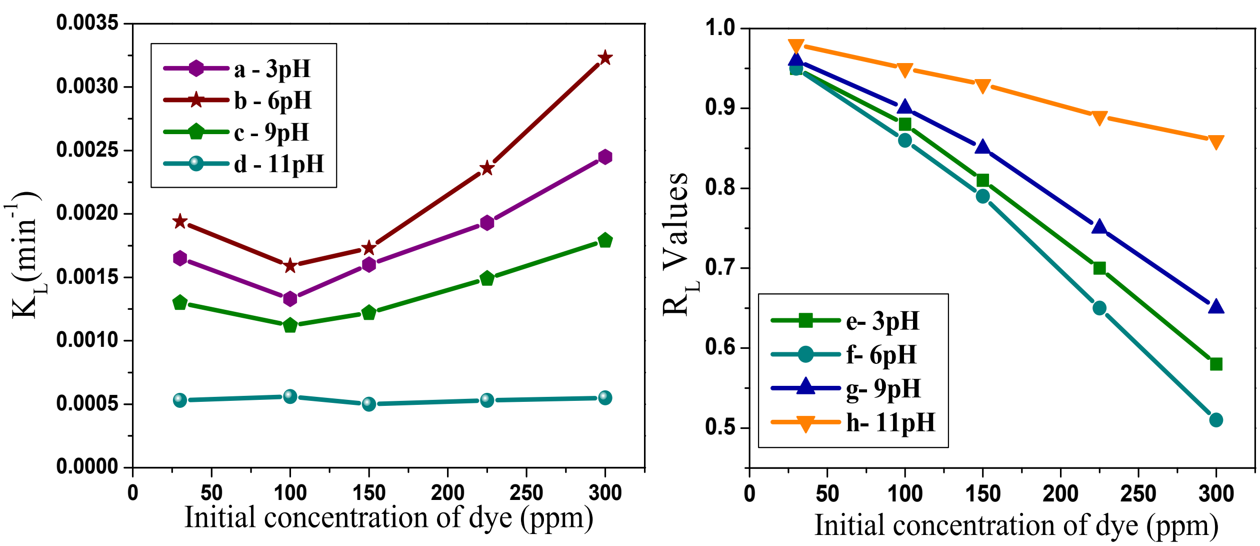

Fig. 6. a-d) Plot of K_L vs concentration of dye and e-f) Plot of R_L vs concentration of dye

2.4. 2. Freundlich Adsorption Model

The adsorption data were fitted in the Freundlich adsorption model using the relation[28]:

$$Ln(q_e) = Ln(K_F) + \frac{1}{n} LnC_e$$

where, K_F is the equilibrium constant of adsorption and 'n' is the adsorption intensity, which indicates the nature of adsorption, whether it is favourable or not. Generally, if the value of 1/n falls in the range of 0.1 to 1.0, it is considered as irreversible adsorption. The Freundlich plot of $Ln(q_e)$ Vs $Ln(C_e)$ is given in **Fig. 7**. From the slope of the curve, the value of 1/n was calculated to be between 0 and 1 (**Fig. 7** (inset)) supporting strong irreversible adsorption on the NFC surface.[29]

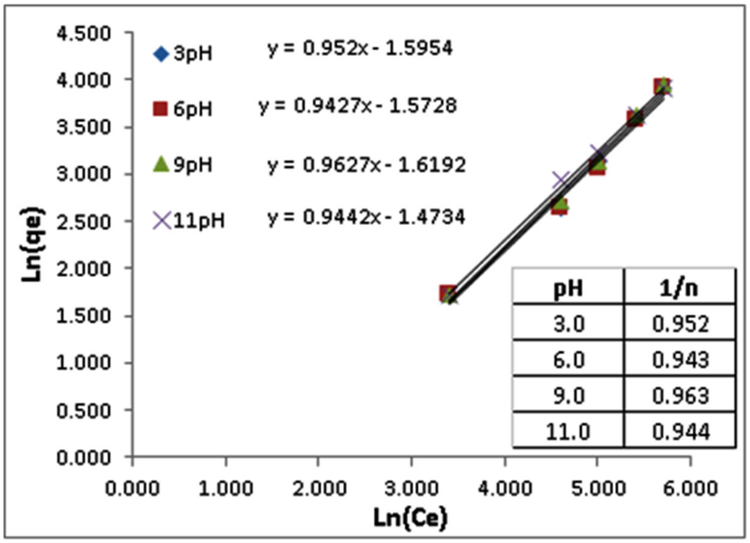

Fig. 7. Freundlich plot of adsorption for different concentrations of pH

2.4.3. Kinetic studies

The adsorption process of methylene blue over NFC was considered as a pseudo-first-order process since the dye was present in large excess in the medium compared to the substrate. The rate equation for the pseudo-first-order adsorption can be given as follows:

$$Ln(q_e - q_t) = Lnq_e - \left(\frac{k_1}{2.303}\right) t,$$

where, q_e is the equilibrium adsorbed quantity of dye, q_t is the quantity of dye adsorbed at a time t and k_1 is the first-order rate constant. A plot of $Ln(q_e - q_t)$ Vs time should give a straight line and the same is given in **Fig. 8**.

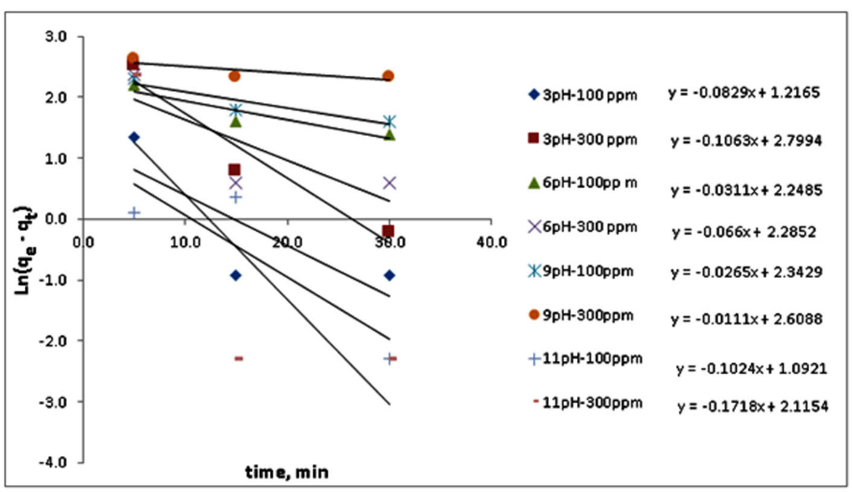

Fig. 8. Pseudo first order kinetics plot of methylene blue adsorption with different concentration over NFC sample.

It can be seen that only a few data were given a straight line, which infers that the adsorption may not follow first-order kinetics. The reason may be due to progressive reduction of dye in the medium due to adsorption, which may deviate from the first-order adsorption. Hence, the adsorption data were substituted into a second-order rate equation which is given by Lagergren *et al.*[30]

$$\frac{t}{q_t} = \frac{1}{k_2 q_e^2} + \left(\frac{1}{q_e}\right) t$$

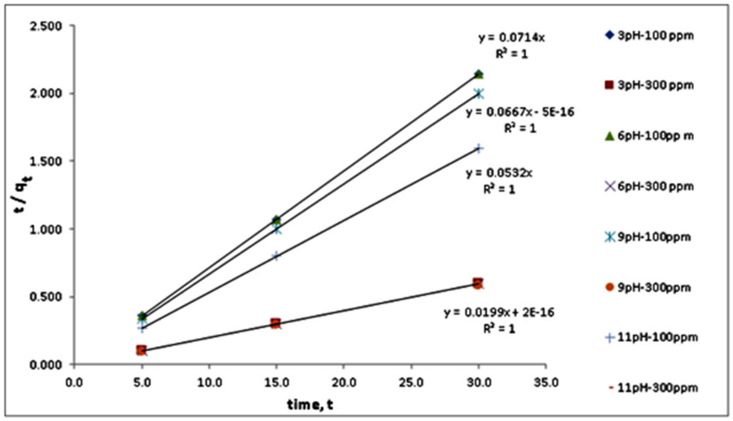

Fig. 9. Second order kinetics plot of methylene blue adsorption with different concentration over NFC sample.

A plot of t/q_e Vs time from the above equation gives a straight line as shown in **Fig. 9** and the R^2 value was 1. The adsorption of dye from the solution containing 300 ppm was found to follow the same trend at all pH, while 100 ppm dye solution followed a similar trend at pH values of 3.0 & 6.0.

2.5. Thermodynamic studies

The adsorption of methylene blue over the NFC was studied at different temperatures, viz., 15 °C, 30 °C and 45 °C. The removal % of the dye at pH=3.0 for different dye concentrations is given in **Figs. 10a-c**.

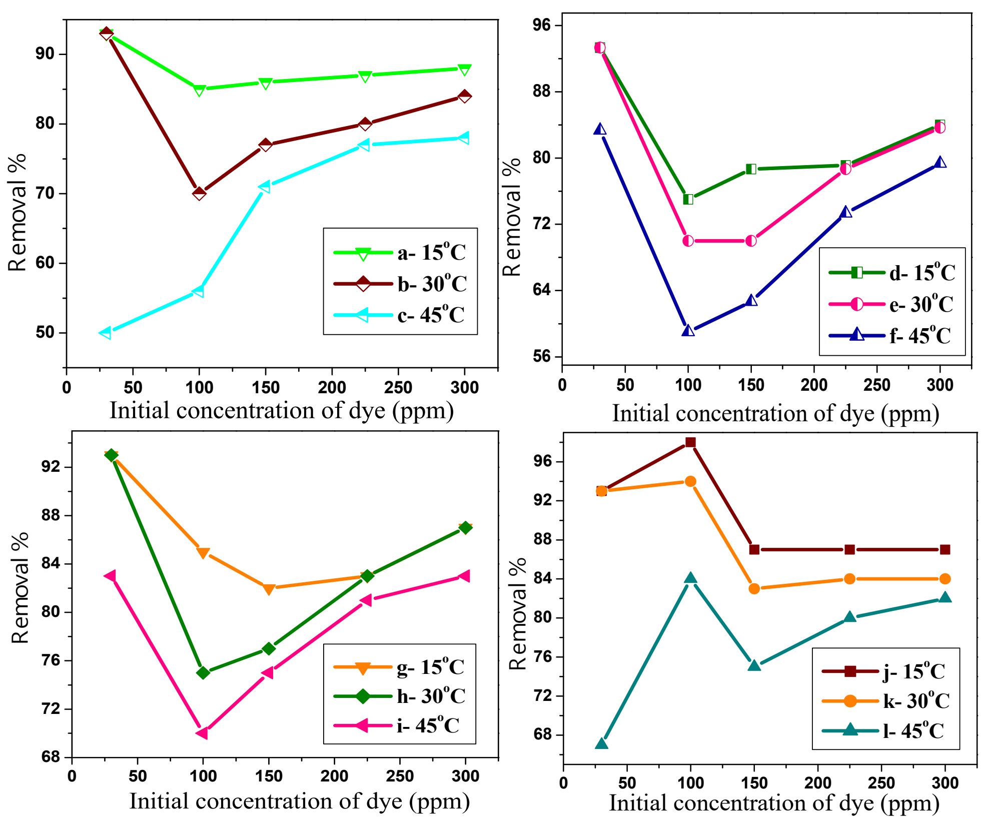

Fig. 10. Dye removal % for different temperatures at a-c) 3 pH, d-f) 6 pH, g-i) 9 pH and j-l) 11 pH

The adsorption was higher at low temperature, suggesting strong physical adsorption since chemisorption is generally favoured at high temperatures[31]. The adsorption of the dye was found to be less at 45 °C as compared to that of 15 °C and

30 °C, which supports the above inference. With the increase in the concentration of dye (300 ppm), the equilibrium adsorption was nearly the same at all temperatures suggesting attainment of saturation adsorption. It was observed that the removal % was found to be saturated above 150 ppm of initial dye concentration. At higher pH 11, the removal % was highest for 100 ppm (**Figs. 10j-l**), suggesting favourable adsorption in alkaline pH at low dye concentration. This is due to the availability of lone pair of electrons over the amine group of chitosan for adsorption in alkaline pH, while the same is converted to onium species in acidic pH. The adsorption at lower initial dye concentration was invariably the same irrespective of pH, suggesting the adsorption of dye may be favoured over the pH insensitive region of NFC surface like hydroxyl groups. This idea is favoured by similarity in adsorption pattern at pH 6 and 9 as shown **Figs. 10d-f** and **g-I** respectively. Even at elevated temperatures, appreciable adsorption was observed in the above pH range.

The rate of adsorption was calculated using second-order kinetics and a plot of ln(k) Vs 1/T from the Arrhenius equation at different pH ranges is given in **Fig. 11**.

$$k = Ae^{-Ea/RT}$$

From the slope, the activation energy of adsorption (ΔG^{+}) can be calculated and the same at different pH is given in **Table 3**. The energy was lowest in the pH range of 6 – 9, suggesting better adsorption as compared to high acidic or alkaline pH (3 or 11). This observation supports the inference made from kinetic studies in the above-said pH range.

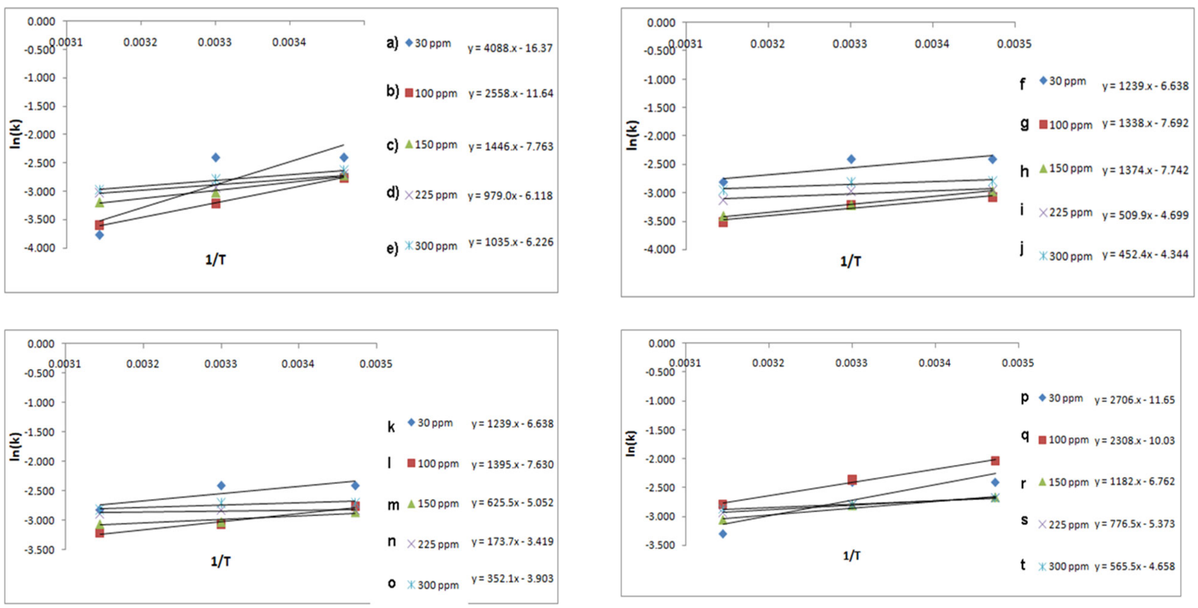

Fig. 11. Arrhenius Plots of methylene blue over for various concentrations of dye at different pH range of a-e) 3 pH, f-j) 6 pH, k-o) 9 pH and p-t) 11 pH

Table. 3. Thermodynamic parameters of adsorption of methylene blue with different initial concentrations over NFC at different pH

			ΔG^{+}		
pH	**30 ppm**	**100 ppm**	**150 ppm**	**225 ppm**	**300 ppm**
3	33.99	21.27	12.02	8.56	8.6
6	10.3	11.12	11.42	4.36	3.76
9	10.3	11.6	5.2	1.44	2.93
11	22.5	19.19	9.83	6.46	4.7
			ΔH^{+}		
pH	**30 ppm**	**100 ppm**	**150 ppm**	**225 ppm**	**300 ppm**
3	36.5	23.78	14.53	11.12	11.12
6	12.81	13.63	13.93	6.9	6.28
9	12.99	14.23	7.75	4.01	5.54
11	25.01	21.7	12.35	8.97	7.22
			ΔS^{+}		
pH	**30 ppm**	**100 ppm**	**150 ppm**	**225 ppm**	**300 ppm**
3	-8.29	-8.29	-8.29	-8.45	-8.31
6	-8.29	-8.29	-8.29	-8.37	-8.31
9	-8.89	-8.7	-8.42	-8.46	-8.62
11	-8.29	-8.29	-8.31	-8.3	-8.3

Similarly, the enthalpy plot of ln(k/T) Vs 1/T was made for different initial concentrations of dye at different pH ranges.[32] The above plots resulted in a straight line as illustrated in **Fig. 12** and the enthalpy change of adsorption (ΔH^{+}) was calculated from the slope (**Table 3**).

The variation of activation energy at different pH for different initial dye concentrations is shown in **Figs. 13 a-e**. Using the thermodynamic relation, $\Delta G^{+} = \Delta H^{+} - T\Delta S$, the entropy change for the adsorption process was calculated and the data is presented in **Table 3**. The process was associated with negative entropy change during adsorption of methylene blue from solution over the NFC surface due to a decrease in disorderness. To find favourable adsorption conditions, the variation of entropy is graphically compared at different pH for different initial dye concentrations as shown in **Figs. 13f-j**.

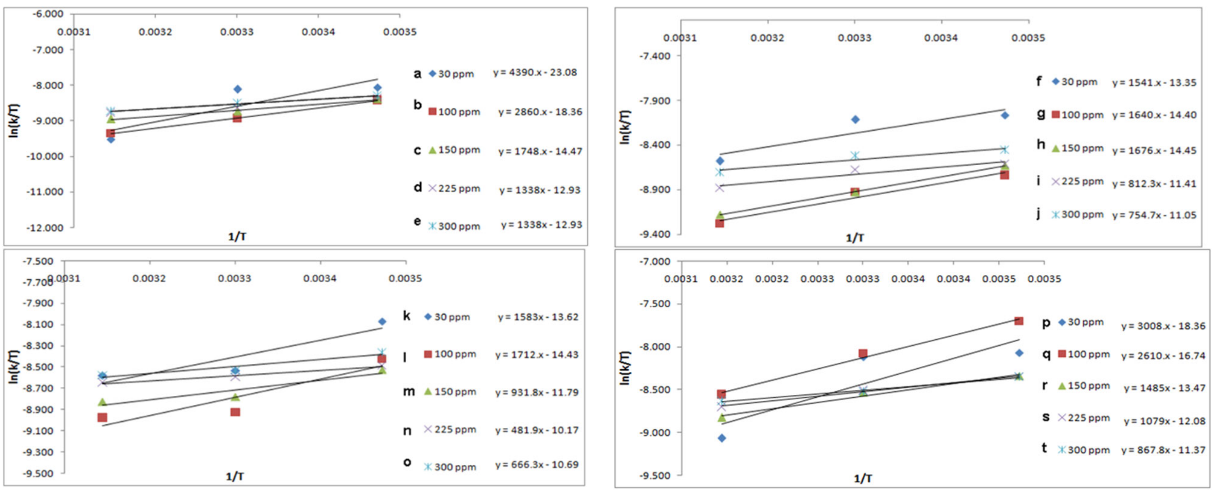

Fig. 12. Enthalpy plots of methylene blue adsorption over NFC for various concentrations of dye at different pH range of a-e) 3 pH, f-j) 6 pH, k-o) 9 pH and p-t) 11 pH

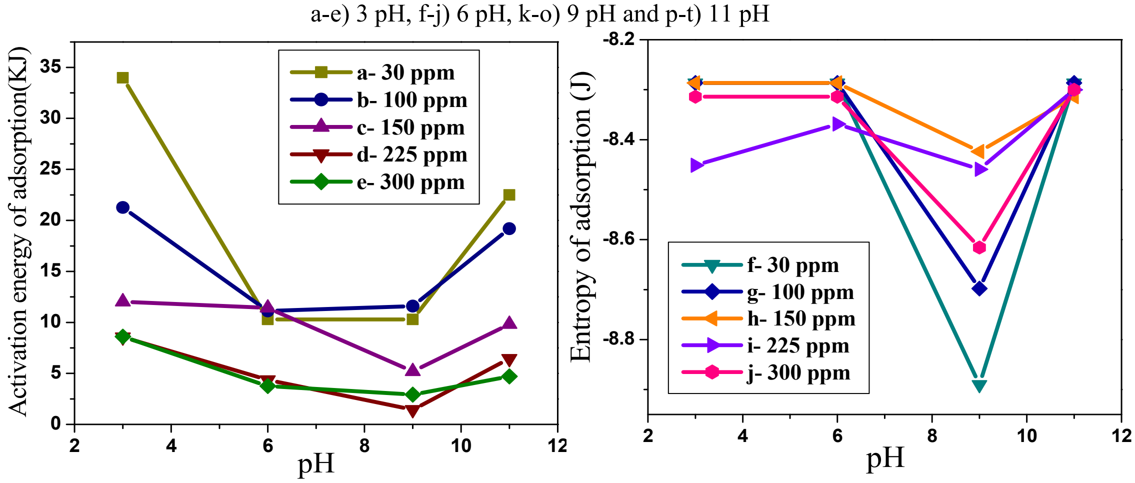

Fig.13. a-e) Variation of activation energy at different pH for different dye concentration and f-j) variation of entropy at different pH for different dye concentration

The entropy change was nearly the same at pH of 3, 6 and 11. At a pH value of 9.0, the entropy reduction was lower suggesting favourable adsorption of dye over the surface and the initial dye concentration of 30 ppm was the lowest. Finally, it can be concluded that a pH of 9.0 is most favourable for the adsorption of methylene blue dye by NFC. The enthalpy of adsorption of methylene blue over neem leaf powder was reported to be 7.37 kJ/mol and the entropy change was reported as 63.36 J/mol.K (positive entropy change).[9] The neem leaf-chitosan adsorption studies report an enthalpy of 22.3 kJ/mol and entropy change of 89 J/mol.K (positive entropy change).[33]

3. Conclusion

The adsorption of methylene blue over chitosan-modified neem flower powder was studied and compared with blank neem flower powder and chitosan-modified neem leaf powder. The chitosan was found to enhance adsorption of methylene blue and the neem flower powder was found to act as a superior adsorbent base as compared to neem leaf powder. The adsorption over the chitosan-modified neem flower was found to be irreversible and the removal rate of the dye from the solution was found to increase with the increase in dye concentration between 6 and 9 pH. The monolayer adsorption capacity was 357 mg/g at 11 pH. The adsorption of dye from solution was found to follow second-order kinetics and found to favour adsorption between pH 6 and 9. Thermodynamic studies revealed that the adsorption process was associated with a decrease in entropy and a pH of 9 was found to be the most favourable condition for adsorption. The activation energy was lowest in the pH range of 6 – 9, suggesting better adsorption as compared to high acidic or alkaline pH (3 or 11).

4. Experimental

4.1. Materials and methods

The chitosan and acetic acid (AR grade) were procured from Merck, India. Methylene blue (MB) dye was obtained from CDH chemicals, India. Neem flowers were collected from our university campus.

4.2. Preparation of NF and NFC

The raw neem flowers were collected and washed with distilled water followed by ethanol and dried at 80^{o}C for 48 h. The dried flowers were grounded into a fine powder with a particle size of approximately 10 to 25 microns. The prepared neem flower (NF) powder was kept in a desiccator to carry out further modification.

The surface NF powder was modified with chitosan to enhance its adsorption potential. 8g of chitosan was dissolved in 1.5 L of distilled water under vigorous stirring. The pH of this colloidal solution was maintained below 6 by adding acetic acid. To this solution, 20 g of NF powder was added and stirred well continuously for 8 h. The modified NF was allowed to stand overnight. The precipitate of chitosan modified NF was filtered and dried in a lyophilizer for 36 h. The chitosan-modified NF (CNF) powder was further studied to assess its adsorption potential towards the cationic methylene blue dye.

4.3. Adsorption Procedure

The methylene blue solution (100 mL) was made into different concentrations in the range of 30 to 300 ppm, and the pH was adjusted between 3 and 11 using hydrochloric acid/sodium hydroxide. The NFC adsorbent was added (0.5g) to the aqueous MB dye solution and the contents were stirred at 250 – 300 rpm. 5 mL of the aliquot was withdrawn from the reaction mixture for every 2 minutes up to 10 minutes and for every 5 minutes from 10 - 30 min and for every 15 minutes from 30 - 60 minutes and centrifuged. The centrifugate was analyzed for absorption at 660 nm using Systronics Type 2202 Double beam spectrophotometer. The dye content in the solution was calculated by comparing it with that standard calibration graph. The adsorption of dye content was calculated from the following equation.

$$q_e = V\frac{C_o - C_e}{w}$$

where q_e is the equilibrium adsorption on dye, C_o is the initial dye concentration, C_e is the concentration of dye in solution after steady-state, V is the total volume of the solution and W is the weight of adsorbent in grams. The removal percentage of (Rem (%)) of dye from the solution by the adsorbent is given by the following equation.

$$Rem(\%) = \frac{(C_o - C_t)}{C_o}\,100$$

4.4. Characterization

The structure of the prepared neem flower and NFC adsorbent was examined by recording their FTIR spectra on Shimadzu 8400S. The micro-textures of the prepared adsorbents were recorded on an SEM instrument. The BET surface area of the adsorbents was evaluated using the Belsorp MR6 instrument from Microtrac and the adsorption data were analyzed using Belsorp Data Analysis Software – Ver. 6.4.1.1.

References

1. Malik P.K. (**2003**) Use of activated carbons prepared from sawdust and rice-husk for adsorption of acid dyes: a case study of Acid Yellow 36. *Dyes Pigments,* 56(3) 239-249. (DOI: 10.1016/S0143-7208(02)00159-6).
2. Hameed B.H., Ahmed A.L., and Latiff K.N.A. (**2007**) Adsorption of basic dye (methylene blue) onto activated carbon prepared from rattan sawdust. *Dyes Pigments*, 75(1) 143-149. (DOI: 10.1016/j.dyepig.2006.05.039).
3. Hayat H., Mahmood Q., Pervez A., Bhatti Z.A., and Baig S.A. (**2015**) Comparative decolorization of dyes in textile wastewater using biological and chemical treatment. *Separation Purif. Technol.,* 154(5) 149–153. (DOI: 10.1016/j.seppur.2015.09.02).
4. Dutta S., Bhattacharyya A., Ganguly A., Gupta S., and Basu S. (**2011**) Application of Response Surface Methodology for preparation of low-cost adsorbent from citrus fruit peel and for removal of Methylene Blue. *Desalination*, 275(1-3) 26-36. (DOI: 10.1016/j.desal.2011.02.057).

5. Suksaroj C., Heran M., Allegre C., and Persin F. (**2005**) Treatment of textile plant effluent by nanofiltration and/or reverse osmosis for water reuse. *Desalination,* 178(1-3) 333-341. (DOI: 10.1016/j.desal.2004.11.043).

6. Torres M.R., Bouzan C. G., and Crespi M. (**2010**) Combination of coagulation–flocculation and nanofiltration techniques for dye removal and water reuse in textile effluents. *Desalination,* 252(1-3) 53-59. (DOI: 10.1016/j.desal.2009.11.002).

7. Bu J., Yuan L., Zhang N., Liu D., Meng Y., and Peng X. (**2020**) High-efficiency adsorption of methylene blue dye from wastewater by a thiosemicarbazide functionalized graphene oxide composite. *Dia. Rel. Materials*, 101,107604. (DOI: https://doi.org/10.1016/j.diamond.2019.107604)

8. He J.S., Cui A., Deng S.H., and Chen J.P. (**2017**) Treatment of methylene blue containing wastewater by a cost-effective micro-scale biochar/polysulfone mixed matrix hollow fiber membrane: performance and mechanism studies. *J. Coll. Interf. Sci.,* 512(15) 190–197. (DOIL 10.1016/j.jcis.2017.09.10).

9. Krishna G., Arunima S. (**2005**) Kinetics and thermodynamics of methylene blue adsorption on neem leaf powder. *Dyes and Pigments,* 65(1) 51-59. (DOI: https://doi.org/10.1016/j.dyepig.2004.06.016)

10. Adeleke J.T., Theivasanthi T., Thiruppathi M., Swaminathan M., Akomolafe T., and Alabi, A.B. (**2018**) Photocatalytic degradation of methylene blue by $ZnO/NiFe_2O_4$ nanoparticles. *Appl. Surf. Sci.,* 455(15) 195–200. (DOI:https://doi.org/10.1016/j.apsusc. 2018.05.184).

11. Shi C.M., Tao F.R., and Cui Y.Z. (**2018**) Evaluation of nitriloacetic acid modified cellulose film on adsorption of methylene blue. *Int. J Biol. Macromol.,* 114(15) 400–407. (DOI: 10.1016/j.ijbiomac.2018.03.146).

12. Patel H., Vashi R.T.A. (**2013**) Comparison study of removal of methylene blue dye by adsorption on neem leaf powder (NLP) and activated NLP. *J. Environ. Engg. Land Mgmt.,* 21(1) 36-41. (DOI: https://doi.org/10.3846/16486897.2012.671772).

13. Srivastava R., Rupainwar D.C. (**2011**) A comparative evaluation for absorption of dye on neem bark and mango bark powder. *Ind. J. Chem. Tech.,* 18(1) 67-75.

14. Srivastava R., Rupainwar D.C. (**2010**) Liquid phase adsorption of indigo carmine and methylene blue on neem bark. *Desal. Water Treat*., 24(1-3) 74-84. (DOI: 10.5004/dwt.2010.1195).

15. Tiwari D.P., Singh S.K., and Neetu, S. (**2015**) Sorption of methylene blue on treated agricultural absorbents: equilibrium and kinetic studies. *App. Wat. Sci.,* 5, 81-88. (DOI: 10.1007/s13201-014-0171-0).

16. Odoemelam S.A., Emeh U.N., and Eddy N.O. (**2018**) Experimental and computational chemistry studies on the removal of methylene blue and malachite green dyes from aqueous solution by (*Azadivachta indica*) leaves. *J. Taibah. Univ. Sci.,* 12(3), 255-265. (DOI: 10.1080/ 16583655.2018.1465725).

17. Munir M., Nazar M.F., Zafar M.N., Zubair M., Ashfaq M., Hosseini-bandegharaei A., Khan S.D., and Ahmad A. (**2020**) Effective adsorption removal of methylene blue from water by didodecyldimetylammonium bromide modified clay. *ACS Omega*, 5(27) 16711–16721. (DOI: 10.1021/acsomega.0c01613).

18. Dülger O., Turak F., Turhan K., and Özgür M. (**2013**) Sumac leaves as a novel low-cost adsorbent for removal of basic dye from aqueous solution. *Inter. Scholar. Res. Not*., 210470 (DOI: 10.1155/2013/210470).

19. Santhi T., Manonmani S., Vasantha V.S., and Chang Y.T. (**2011**) A new alternative adsorbent for the removal of cationic dyes from aqueous media. *Arab. J. Chem.* 9(1) 466-474. (DOIL 10.1016/j.arabjc.2011.06.004).

20. Danish M., Ahmad T., Nadhari W.N.A.W., Ahmad M., Khanday W.A., Ziyang L., Pin Z. (**2018**) Optimization of banana truck activated carbon production for methylene blue-contaminated water treatment. *App. Wat. Sci*., 8(1) 9-12. (DOI: https://doi.org/10.1007/s13201-018-0644-7).

21. Li Y., Wang S., Shen Z., Li X., Zhou Q., Sun Y., Wang T., Liu Y., and Gao Q. (**2020**) Gradient adsorption of methylene blue and crystal violet onto compound microporous silica from aqueous medium. *ACS Omega,* 5(43) 28382–28392. (DOI: https://doi.org/10.1021/acsomega.0c04437).

22. Smith B.C. (**2017**) An IR Spectral Interpretation Potpourri: Carbohydrates and Alkynes. *Spectroscopy*, 32, 18–24.

23. Sneddon G., Alexey Y.G., Humphrey Y.H.P. (**2015**) Sustainable CO_2 Adsorbents Prepared by Coating Chitosan onto Mesoporous Silicas for Large-Scale Carbon Capture Technology. *Ener Tech*., 3(3) 249 – 258. (DOI: https://doi.org/10.1002/ente.201402211).

24. Kuang Y., Xiaoping Z., and Shaoqi Z. (**2020**). Adsorption of Methylene Blue in Water onto Activated Carbon by Surfactant Modification. *Water,* 12(2) 587-589. (DOI: 10.3390/w12020587).

25. Heraldy, P.E., Hidayat, Y., & Firdaus, M. (2015). The langmuir isotherm adsorption equation: The monolayer approach. IOP Conf Series: *Mater Sci Engg*., 107,8–9.

26. Priyadarshini B., Tanaswini P., Tapas R.S. (**2020**) An efficient and comparative adsorption of Congo red and Trypan blue dyes on MgO nanoparticles: Kinetics, thermodynamics and isotherm studies. *J. Magnesium Alloys,* 9(2) 478-488. (DOI: https://doi.org/10.1016/j.jma.2020.09.004).

27. Meroufel B., Benali O., Benyahia M., Benmoussa Y., and Zenasni M.A. (**2013**) Adsorptive removal of anionic dye from aqueous solutions by Algerian kaolin: Characteristics, isotherm, kinetic and thermodynamic studies. *J. Mater Environ. Sci.* 4(3) 482-491.

28. Revathi H., Kaviyarasu A., Murugan T., Dinesh Kumar M., and Sharmila Devi R. (**2018**) Adsorption isotherm and kinetic studies onto removal of reactive yellow -14 dye by using ixora coccinea leaf powder. *Rasayan J. Chem.* 11(4) 1415-1422. (DOI: 10.31788/ RJC.2018.1143054).

29. Youcef L.D., Lala S.B., and Alberto L.G. (**2019**) Adsorption of a cationic methylene blue dye on an Algerian palygorskite. *App. Clay Sci.* 179, 105145. (DOI: 10.1016/j.clay.2019.105145).

30. Lagergren S. (**1898**) Zur theorie der sogenannten adsorption gelöster stoffe, Kungliga Svenska Vetenskapsakademiens. *Handlingar,* 24, 1-39.

31. Herrero E., Juan M.F., Sonia B., Zorana R., and Gregory J. (**2000**) Temperature Dependence of CO Chemisorption and Its Oxidative Desorption on the Pt(111) Electrode. *Langmuir,* 16(11) 4779–4783. (DOI: https://doi.org/10.1021/la9907432).
32. Ratheshkumar P., Induja S., and Raghavan P.S. (**2020**) Selective Catalytic Oxidation of Organic Sulfides to Sulfoxides without Forming Sulfones over Solid Molybdenum Blue: Kinetic and Thermodynamic Studies. *Asian J. Chem.*, 32, 2267-2274. (DOI: 10.14233/ajchem.2020.22789).
33. Francis O.A., Ahmad Zaini M.A., Misau Idris M., Abdulsalam S., and Aliyu Usman E. (**2019**) Methylene Blue Adsorption onto Neem Leave/Chitosan Aggregates: Isotherm, Kinetics and Thermodynamics Studies. *Int. J. Chem. Reac. Eng.,* 18(1), 20190093. DOI: 10.1515/ijcre-2019-0093).